Electronic Supplementary Material (ESI) for Energy & Environmental Science.
This journal is © The Royal Society of Chemistry 2024

Supporting Information

Visualizing the SEI Formation Between Lithium Metal and Solid-State Electrolyte

Fucheng Ren, [a] Yuqi Wu, [a] Wenhua Zuo, [b] Wengao Zhao, * [c] Siyuan Pan, [d] Hongxin Lin, [d] Haichuan Yu, [e] Jing Lin, [c] Min Lin, [d] Xiayin Yao, [e] Torsten Brezesinski, [c] Zhengliang Gong*[a] and Yong Yang*[a, d]

[a] College of Energy, Xiamen University, Xiamen 361102, China.
E-mail: zlgong@xmu.edu.cn

[b] Chemical Sciences and Engineering Division, Argonne National Laboratory, Lemont, IL, 60439, USA.

[c] Institute of Nanotechnology, Karlsruhe Institute of Technology (KIT), 76344 Eggenstein-Leopoldshafen, Germany.
E-mail: wengao.zhao@kit.edu

[d] State Key Laboratory for Physical Chemistry of Solid Surface, Department of Chemistry, College of Chemistry and Chemical Engineering, Xiamen University, Xiamen 361005, China.
E-mail: yyang@xmu.edu.cn

[e] Ningbo Institute of Materials Technology and Engineering, Chinese Academy of Sciences, Ningbo315201, P.R. China.

Electrochemical stability: The electrochemical window of electrolyte is evaluated by constructing the grand potential phase diagram of specific phase with the composition *C* at the chemical potential of Li (μ_{Li}). The energy minimum $E_{eq}(C)$ is identified by comparing the energy of all relevant phases in the compositional space. The decomposition energy at a given chemical potential of μ_{Li} is calculated as follows:

$$\Delta E_{D}^{open}(phase, \mu_{Li}) = E_{eq}\left(C_{eq}(C,\mu_{Li})\right) - E(phase) - n_{Li} \cdot \mu_{Li} \quad (1)$$

Here, the chemical potential of μ_{Li} is referenced to lithium metal.

Density functional theory (DFT) calculations: All DFT calculations are performed by the Vienna ab initio simulation (VASP) package.[1] The projector augmented wave (PAW)[2,3] method and Perdew-Burke-Ernzerhof functional (PBE)[4,5] were used throughout all calculations. The plane wave basis cutoff is set to be 520 eV. The convergence criterion of energy and force is 10^{-5} eV and 0.001 eV/Å. To ensure the same *k*-point grid for all systems, the Brillouin zone samplings were controlled by KSPACING, which is set to be 0.5.

Deep potential generation (DP-GEN): To generate a potential of the solid-solid reactive interface model, the descriptions for the bulk of the electrode/electrolyte and interphase layer must be contained, simultaneously. Hence, the generation of the deep potential of reactive interface model Li(001)|β-Li_3PS_4(100/010/001) is divided into two steps, as shown in Figure 1. Step 1: Generating the bulk descriptors for the Li-metal electrode and β-Li_3PS_4 SSE. Step 2: Generating the descriptors for the reactive interface model of Li(001)|β-Li_3PS_4(100/010/001) containing the bulk description of lithium anode and β-Li_3PS_4 SSE and interphases formed between them. The bulk training dataset of Li and Li_3PS_4 is integrated for initialization of step 2 in order to obtain the deep potential of the reactive interface model.

Note that the bulk Li with space group $Im\bar{3}m$ (bcc structure, mp-135) possesses the same structure at the crystal surface of (100), (010), and (001), as shown in **Figure S1**.

Herein, the (001) surface was selected to construct the reactive interface model. For β-Li_3PS_4, Li^+ prefers to migrate along the [010] direction,[2] thus the (010) surface was selected. Additionally, another two low miller index surfaces of β-Li_3PS_4 (100) and (001) with smaller lattice mismatch with Li-metal (001) surface[3] were also selected to construct the interfacial model (see **Fig. S1c**) for investigating the interfacial reaction between Li-metal and β-Li_3PS_4.

Initial dataset: Ab-initio molecular dynamics (AIMD) calculations with trajectories of 15 ps at 400 K is used to generate the initial dataset for the bulk training of lithium metal and β-Li_3PS_4 (step 1), as well as the reactive interface mode of Li(001)|β-Li_3PS_4(100/010/001). A supper cell of 3×3×3 and 1×1×2 was built for the bulk of Li and β-Li_3PS_4, respectively. The interface models of Li(001)|β-Li_3PS_4(100/010/001) are shown in **Figure S1**. In all AIMD simulations, the DFT-based force evaluations were spin-polarized with a single Γ-center *k*-point grid. A 1 fs time step was applied in all AIMD simulations. NVT ensemble using a Nose-Hoover thermostat was employed for AIMD simulation. A Verlet algorithm was used to integrate the Newton's equation of motion. Finally, the AIMD simulation results are converted into the recognizable data type of DP-training containing the energy and force information by dpdata software. [6]

DP-GEN iterations: The deep potential of the reactive interface model was generated by DG-GEN,[6] which consists of a series of training, exploration, and labeling iterations as shown in Figure 1. In the first iteration, the initial datasets obtained from initialization (energy and force information of configurations) are used and trained with different random seeds in the training stage by DeePMD-kit.[7-8] Four models are obtained and used in the exploration stage. The embedding network has three layers with 25, 50, and 100 nodes, and the fitting network is composed of three layers, each of which has 240 nodes used in the training stage.[7] The loss function with an exponential decay-learning rate was set from 5×10^{-3} to 4×10^{-8}.

In the exploration stage, several NPT ensembled MD simulations using the DP model

obtained from the training stage are performed at different thermodynamic conditions using the LAMMPS software. The DeePMD exploration time is prolonged from 20 ps to 200 ps. The temperature and pressure ranges from 200 to 1000 K and 0 to 100 bar, respectively. The configurations in DeePMD trajectories are selected according to the model deviation defined by the maximum deviation of force (σ_i^{max}) on atom i between DP models:

$$\sigma_i^{max} = max_i\sqrt{\langle\|F_i(R_t) - \langle F_i(R_t)\rangle\|\rangle^2} \quad (2)$$

where $F_i(R_t)$ is force on atom i, and $\langle F_i(R_t)\rangle$ is the average force on atom i using the four DP models. For the atom i with the largest force deviation that can represent the deviation of the model, once σ_i^{max} reaches the convergency accuracy, the force of other atoms has converged. The configurations with force deviation $\sigma_i^{max} < \sigma_{low}$ or $\sigma_i^{max} > \sigma_{high}$ are discarded, only the configurations with force deviation $\sigma_{low} < \sigma_i^{max} < \sigma_{high}$ are labeled as candidates. σ_{low} and σ_{high} are set to be 0.08 and 0.2 eV/Å for the bulk system of lithium and β-Li_3PS_4, 0.15 and 0.4 eV/Å for reactive interface model of Li(001)|β-Li_3PS_4(100/010/001), respectively. Then, the candidates are labeled and added to the next training step. The whole iterations run until 99% of explored configurations reach the model deviation $\sigma_i^{max} < \sigma_{low}$.

The labeling of the candidates is accomplished in the VASP package, and all the setting parameters are the same as described in the DFT calculation details.

Finally, 7150 candidates are collected in total, and the training of the interface model (step 2) undergoes 22 iterations. The deep potential model was trained with 2×10^6 steps using all collected configurations containing the bulk database (Li-metal: 8 iterations and 1157 configurations, 9 iterations and 1707 configuration) and interfacial database (Li|β-Li_3PS_4: 22 iterations and 4286 interfacial configurations) to minimize the error of total energy.

Deep potential molecular dynamics (DeePMD) simulations: The initial structures of

the reactive interface model for Li(001)|β-Li_3PS_4(100/010/001) are built, and the box sizes are 26.29×25.37×387.89 $Å^3$ for Li(001)|β-Li_3PS_4(001) (12240 atoms), 31.62×31.01×409.33 $Å^3$ for Li(001)|β-Li_3PS_4(100) (19060 atoms), and 24.95×26.15×404.28 $Å^3$ for Li(001)|β-Li_3PS_4(010) (12160 atoms). The size along the *z*-axis is large enough to exclude boundary effects toward the interface reactions. The DeePMD simulations are performed within the LAMMPS software package using the well-trained DP-model.[9-10] 3D periodic conditions are applied. The atoms at the bottom (β-Li_3PS_4) and top (Li) of the interface model (1 nm thickness) are fixed to ensure there is only one reactive interface, where reactions can take place in each model. The isothermal-isobaric ensemble (NPT) with Nose-hoover thermostat is used throughout the simulations. When pressure is computed (hydrostatic pressure), all three diagonal components together dilate/contract the dimensions. The DeePMD simulations are performed at 300, 400, and 600 K, and the pressure is set to be 0 or 100 bar to study temperature and pressure effects on the interface reaction. The total time duration of all simulations is 2 ns. A time step of 1 fs is used to integrate Newton's equations of motion. All trajectory profiles are analyzed using the OVITO visualization software.[11]

Diffusion coefficient calculation: To gain more insight into the kinetics of Li|β-Li_3PS_4 interfacial reactions, the lithium, phosphorus, and sulfur diffusion coefficients during the whole process were calculated from the mean squared displacement (MSD), containing the mutual ion diffusion, Li_2S nucleation, growth and stabilization stages. The related equation is shown in the following:

$$MSD = \frac{1}{N}\sum_{i=1}^{N}\left\langle\left[r_i(\Delta t + t_0)\right] - \left[r_i(t_0)\right]\right\rangle^2 \quad (3)$$

where N is the total number of ions that are assumed to be the mobile carriers contributing to diffusion. $\left[r_i(\Delta t + t_0)\right] - \left[r_i(t_0)\right]$ is the displacement of the i-th ion in the time interval of Δt. The diffusion coefficients were calculated using the following equation:

$$D = \frac{1}{6} \times \frac{dMSD}{d\Delta t} \qquad (4)$$

The diffusion dimension in the interface model is regarded as 3D.

Fabrication of Li|β-Li_3PS_4|Cu all solid-state batteries: 100 mg β-Li_3PS_4 powder was pressed into pellet with the pressure of 360 MPa to obtain SSEs layer. Li/β-Li_3PS_4/Cu cell were assembled by attaching Li metal and Cu current collector on each side of the β-Li_3PS_4 pellet and pressing them with the pressure of 50 MPa. The cell was evaluated with LAND CT-2991A (Wuhan, China) test system. The Li-metal plating current density was set at 0.05 mA cm^{-2} for 80 hours.

Solid state nuclear magnetic resonance (SS-NMR): Ex-situ ^{7}Li and ^{31}P magic-angle spinning (MAS) NMR spectroscopy were acquired on a Bruker AVANCE III 400 MHz spectrometer. All experiments were carried out using a double resonance 1.3 mm MAS probe, spinning at frequencies up to 50 kHz with a single pulse sequence (90° pulse and 30° pulse for ^{7}Li and ^{31}P, respectively). For ^{7}Li MAS NMR, the 90° pulse length was 1.47 μs and with a recycle delay of 2 s. The ^{7}Li shifts were referenced to LiF (-1 ppm), at a ^{7}Li Larmor frequency of 155.53 MHz. For ^{31}P MAS NMR, the 30° pulse length was 0.53 μs and the recycle delay was 1 s. The ^{31}P shifts were referenced to ADP (1 ppm), at a ^{31}P Larmor frequency of 162.02 MHz.

The time-of-flight secondary ion mass spectrometry (ToF-SIMS): To investigate the distribution of interpfacial species, the ToF-SIMS (TOF-SIMS, IONTOFM6, Germany) equipped with a 25 kV Bi cluster primary-ion gun was used for the analysis and a dual-source column was conducted for Cs^{+} depth profiling measurements.

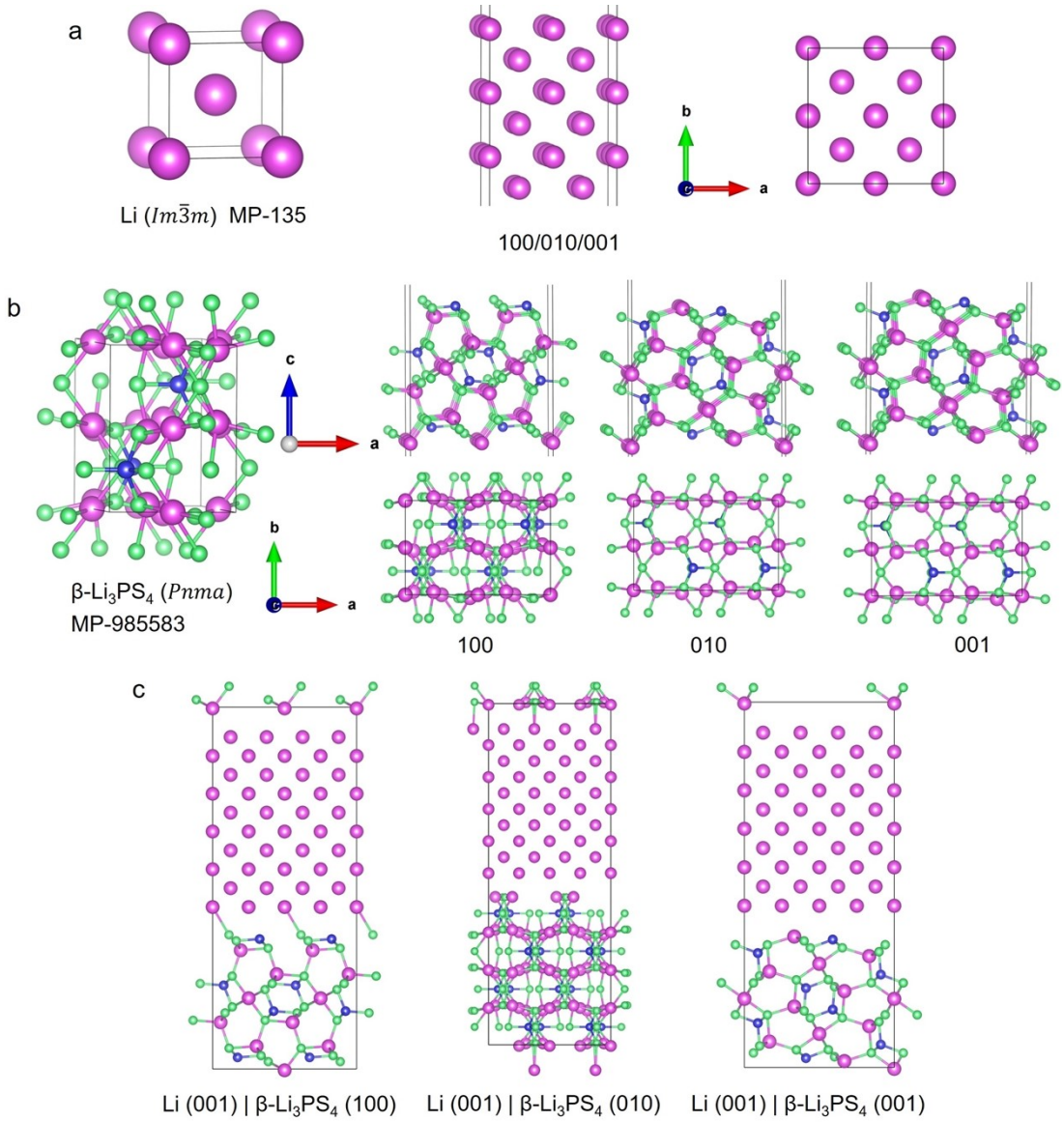

Fig. S1 Surface structure of (a) Li(100)/(010)/(001) and (b) β-Li_3PS_4(100)/(010)/(001). (c) Reactive interface model of Li(001)|β-Li_3PS_4(100)/(010)/(001). Li, S, and P atoms are shown in pink, green, and blue, respectively.

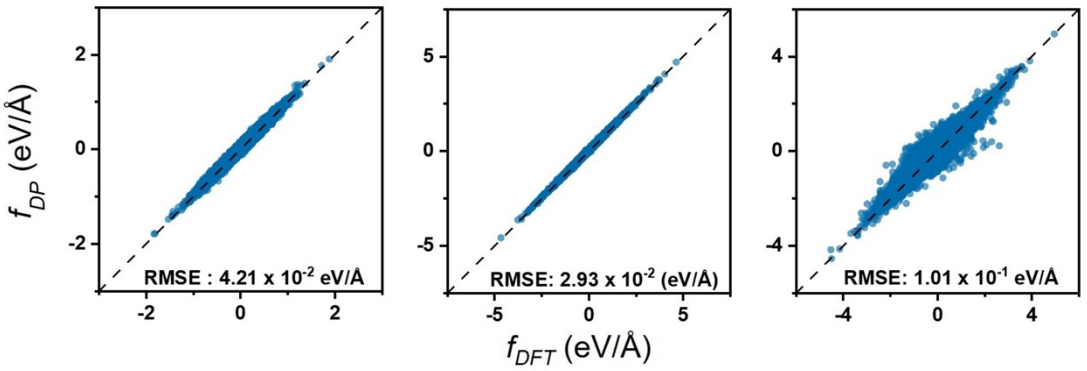

Fig. S2 Comparison of forces of structures predicted by DFT and DP for Li (left), β-Li_3PS_4 (middle), and Li|β-Li_3PS_4 (right).

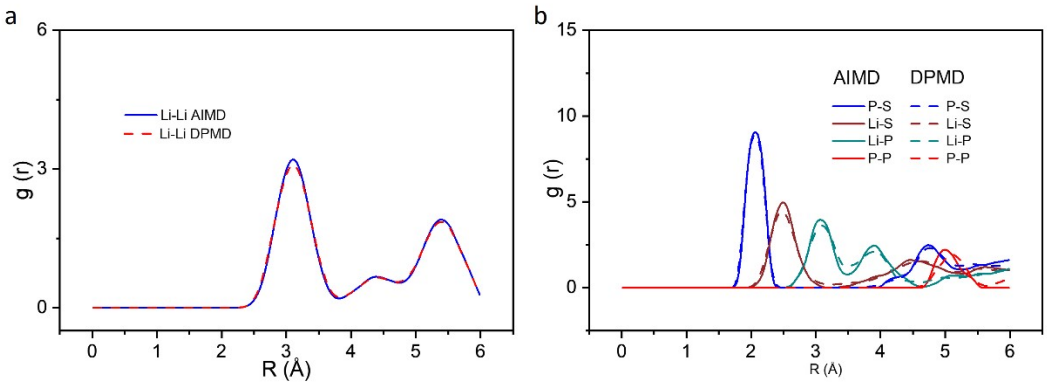

Fig. S3 RDF curves for (a) lithium metal and (b) β-Li_3PS_4 obtained from DeePMD (dotted line) and AIMD (solid line) simulations.

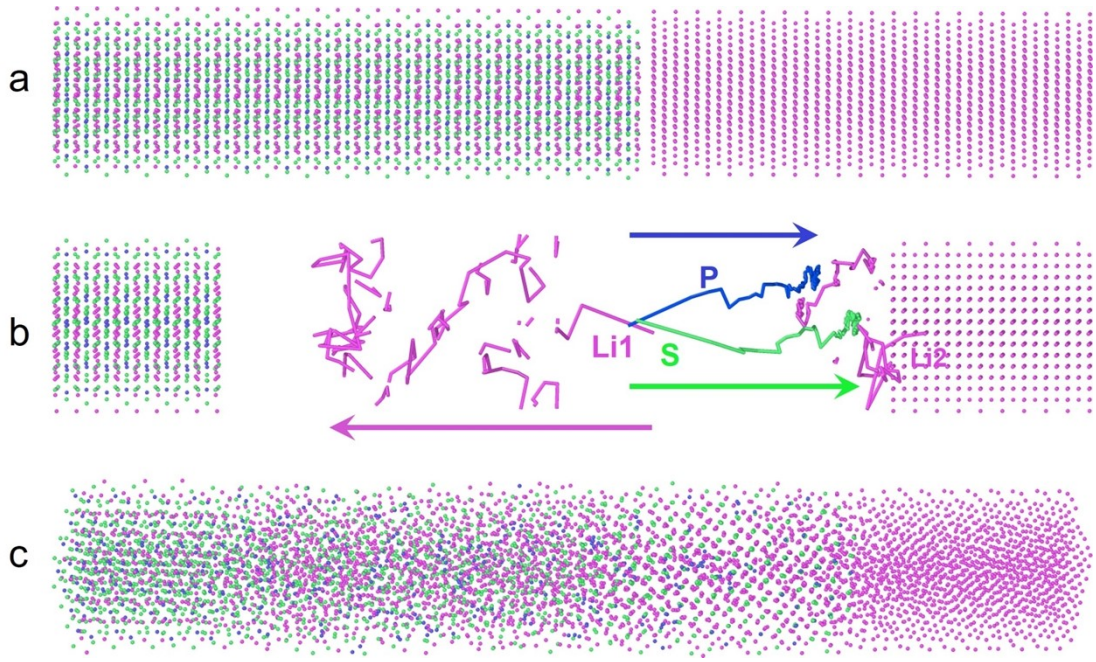

Fig. S4 (a) Initial structure of the interface model. (b) Evolution trajectory of lithium (Li1 close to the interface, Li2 far away from the interface), phosphorus, and sulfur ions. (c) Final structure of the interface model.

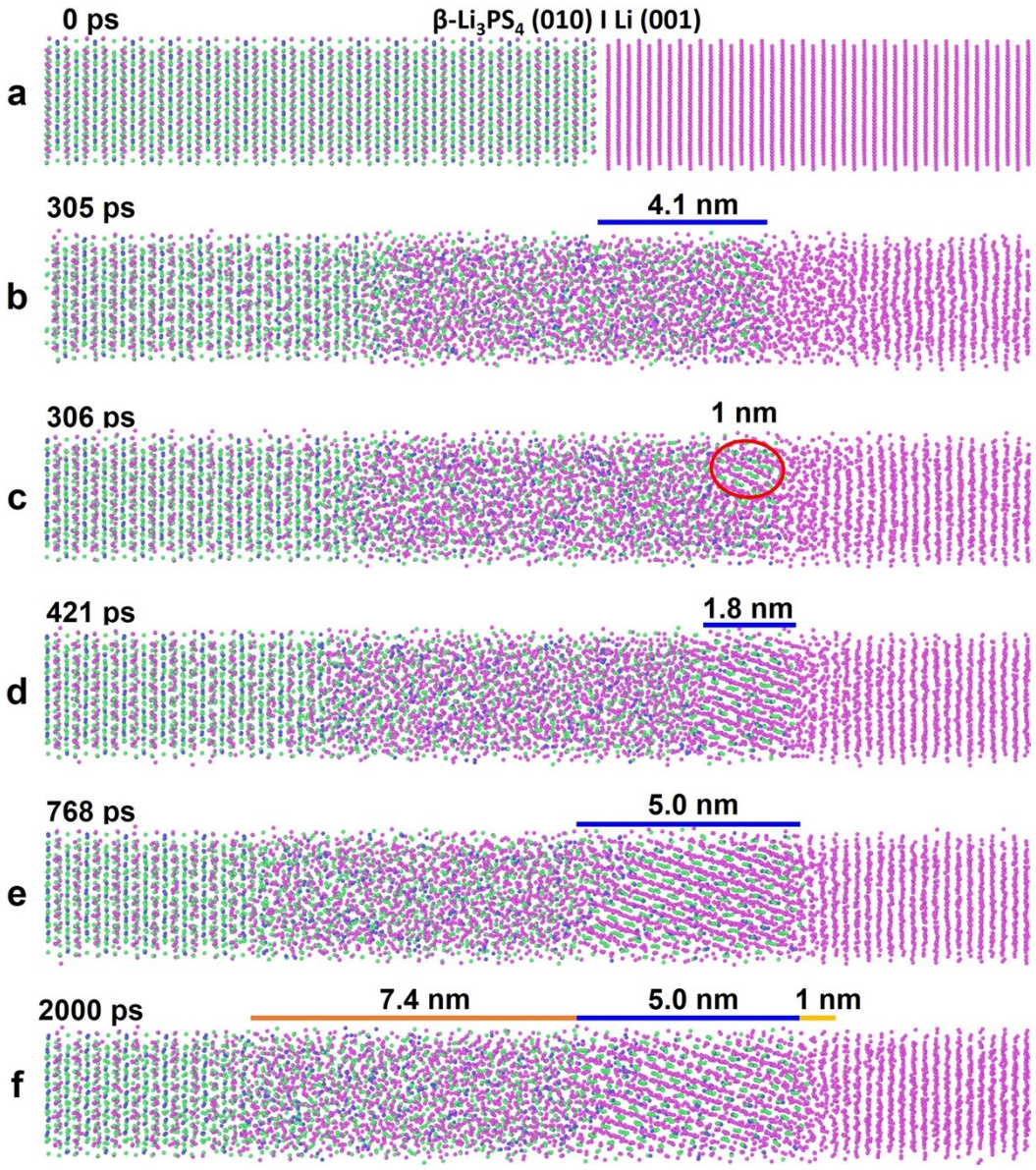

Fig. S5 Interface structures for Li(001)|β-Li_3PS_4(010) at different simulation times. (a, b) Ion diffusion, (c, d) nucleation, (d, e) growth of crystalline phase, and (e, f) stabilization of SEI layer.

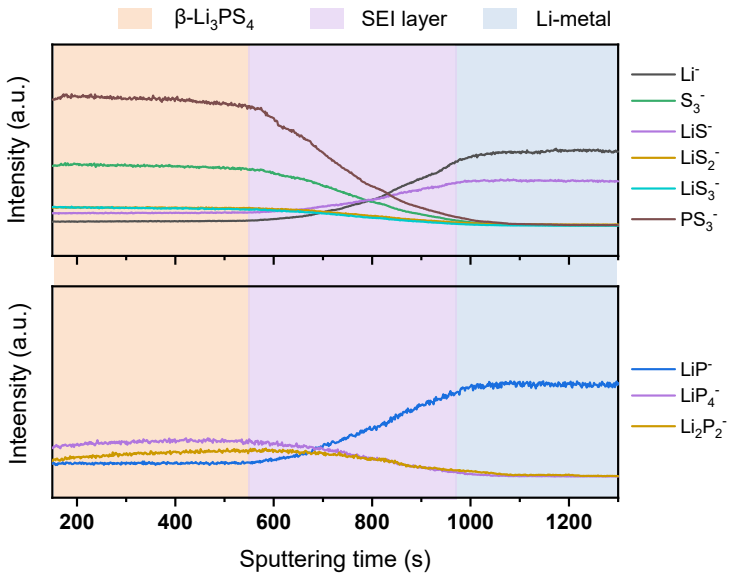

Fig. S6 ToF-SIMS depth profiles of Li|β-Li_3PS_4|Cu ASSB after plating Li for 80 hours at 0.05mA cm^{-2}.

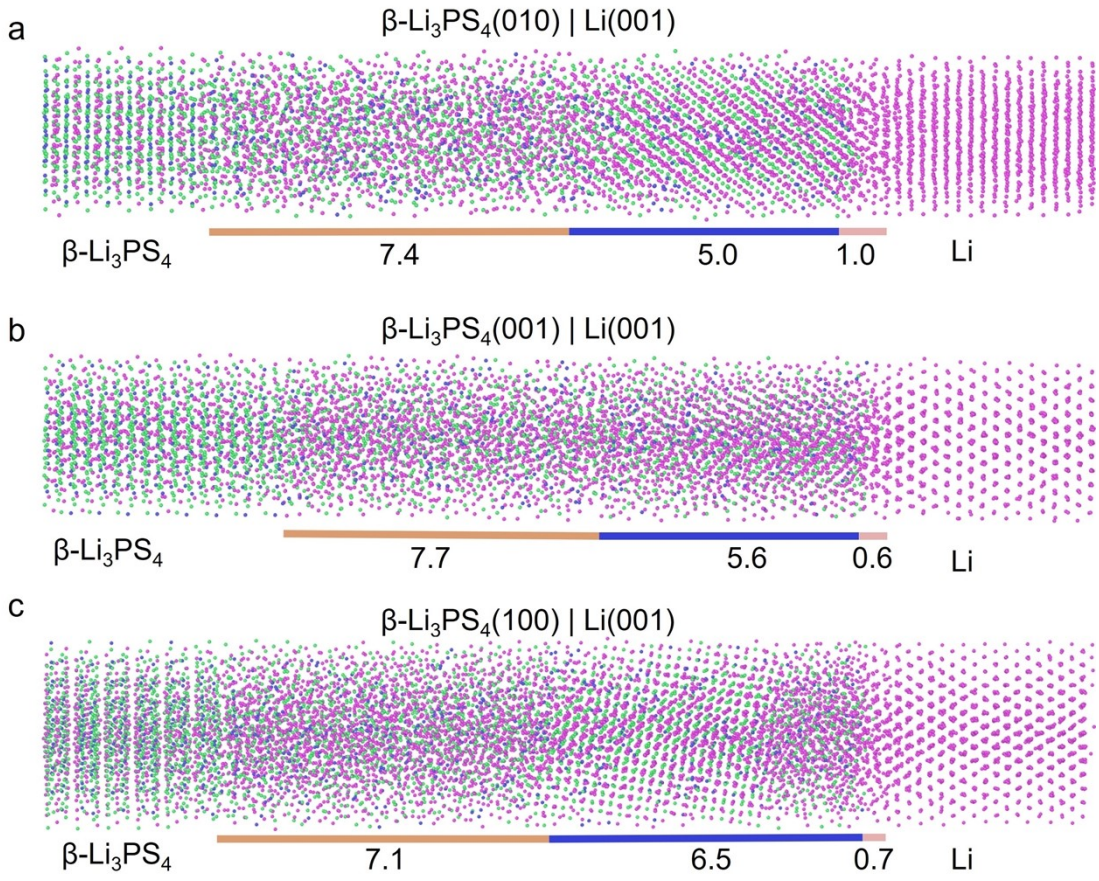

Fig. S7 Structure of the SEI formed between Li and β-Li_3PS_4 at 300 K and 100 bar. (a) Li(001)|β-Li_3PS_4(010), (b) Li(001)|β-Li_3PS_4(001), and (c) Li(001)|β-Li_3PS_4(100). The thickness of each region is given in units of nm.

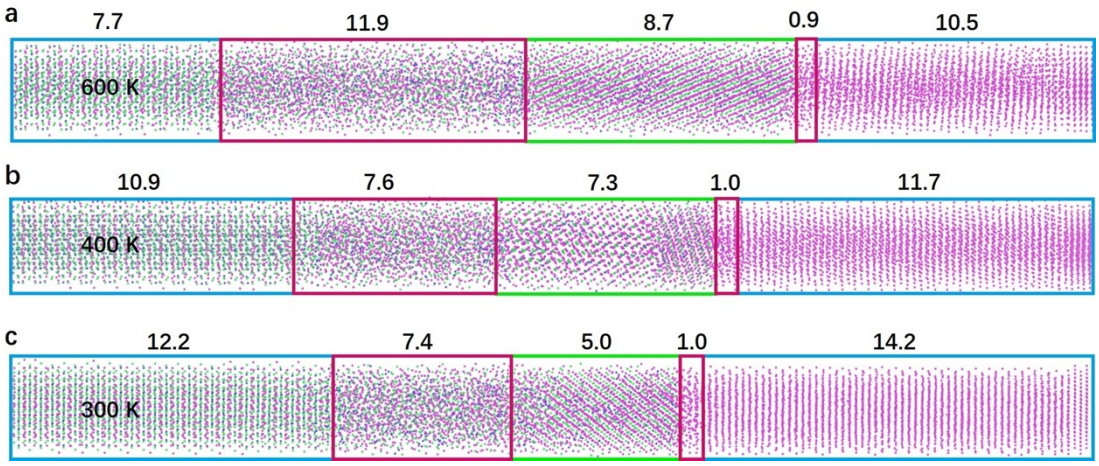

Fig. S8 Schematic of the final interface structure between Li(001) and β-Li_3PS_4(010) at (a) 600 K, (b) 400 K, and (c) 300 K and 100 bar. The thickness of each region is given in units of nm.

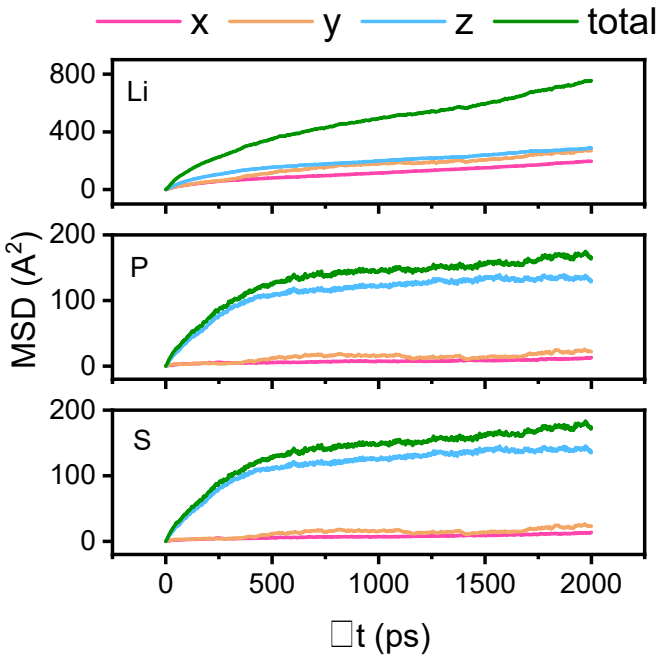

Fig. S9 MSD of (a) lithium, (b) phosphorus, and (c) sulfur ions along the *x*-, *y*-, and *z*-direction as a function of Δt in the interface model of Li(001)|β-Li_3PS_4(010) from DeePMD simulations over 2000 ps at 300 K and 100 bar.

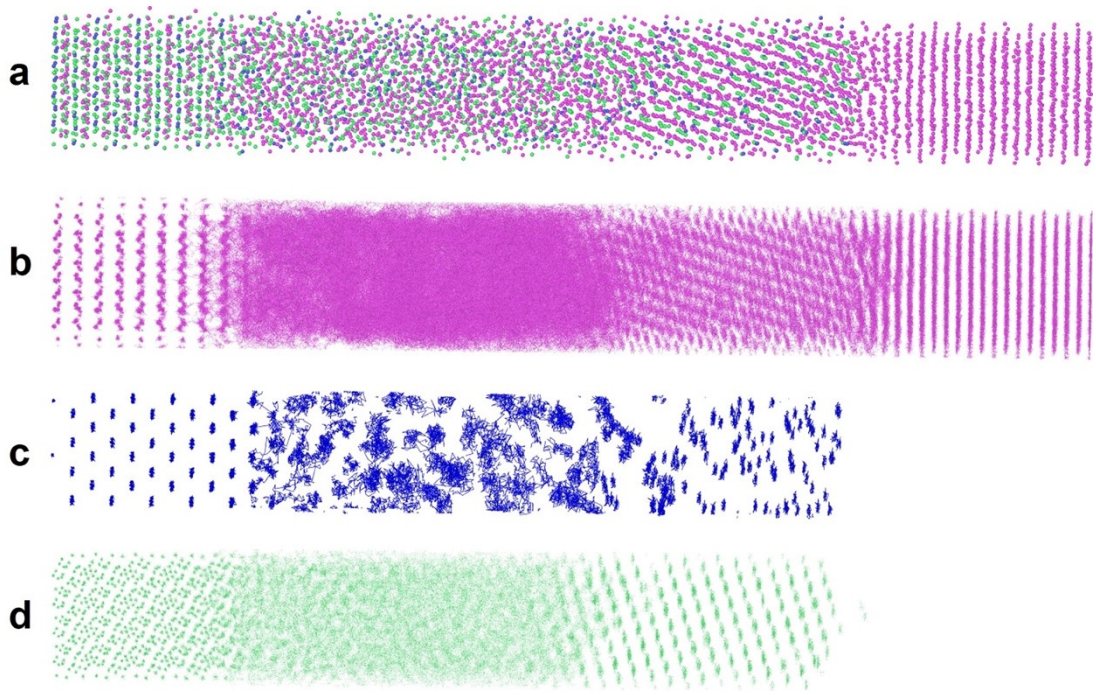

Fig. S10 (a) Final interface structure of Li(001)|β-Li_3PS_4(010). Trajectories from DeePMD simulations generated in the last 500 ps (1500-2000 ps) for (b) lithium, (c) phosphorus and (d) sulfur at 300 K and 100 bar.

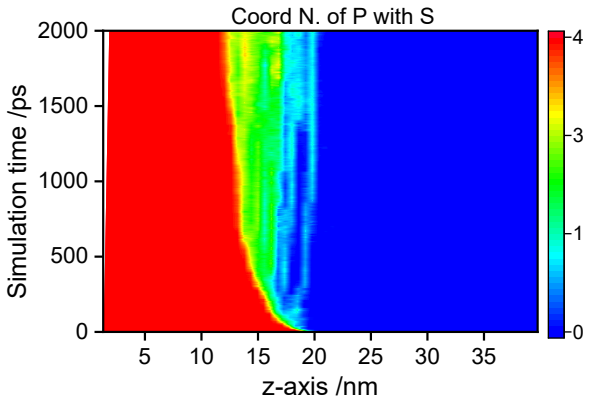

Fig. S11 The coordination number of phosphorus with sulfur in the interface model of Li(100)|β-Li_3PS_4(010) at 300 K and 100 bar.

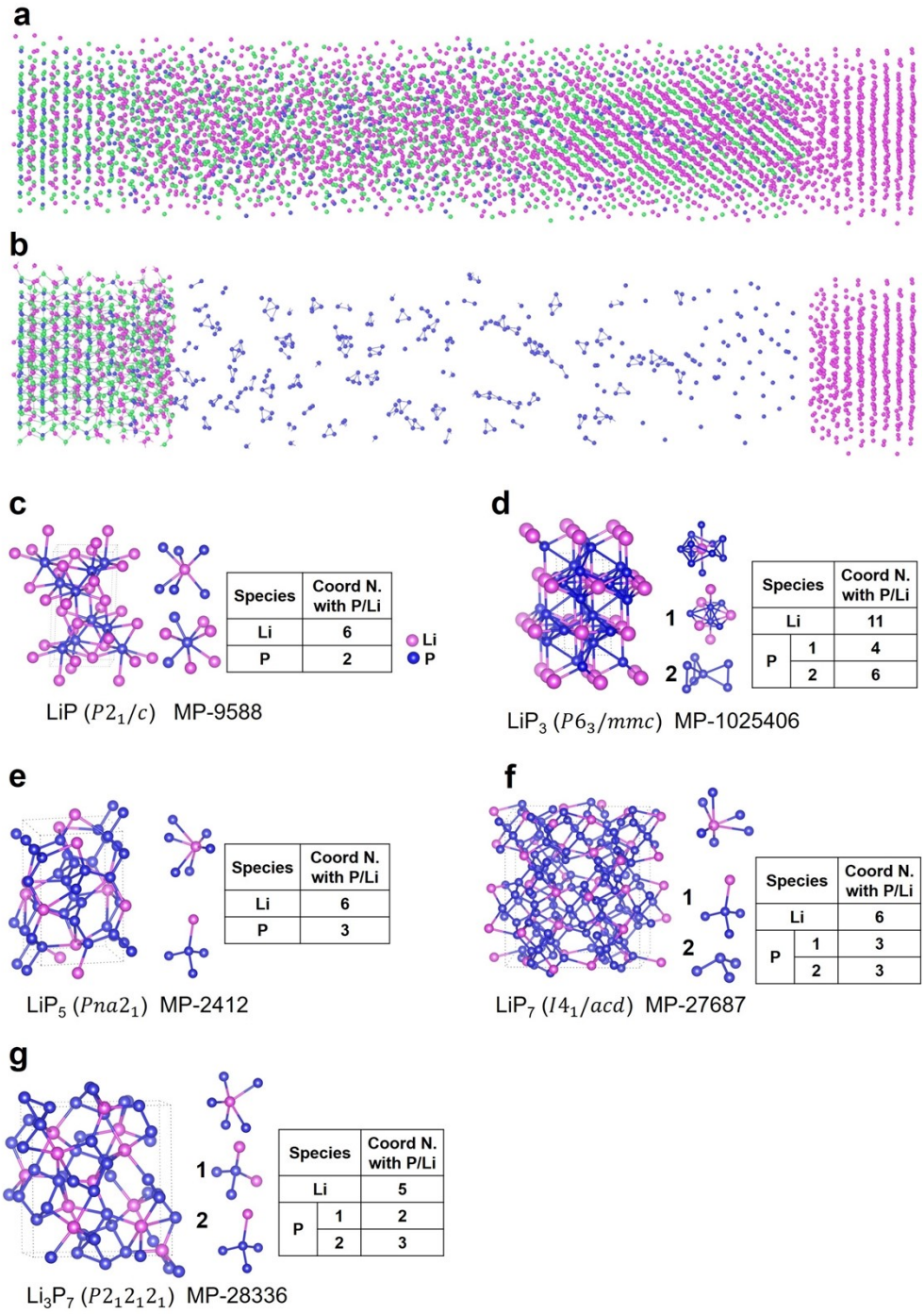

Fig. S12 (a) The distribution of phosphorus and sulfur in the SEI layer. (b) Phosphorus distribution and coordination environment with phosphorus. (c-f) Crystal structures of LiP, LiP_3, LiP_5, LiP_7, and Li_3P_7 and corresponding coordination number of lithium and phosphorus with phosphorus and lithium. Li, S, and P atoms are shown in pink, green, and blue, respectively.

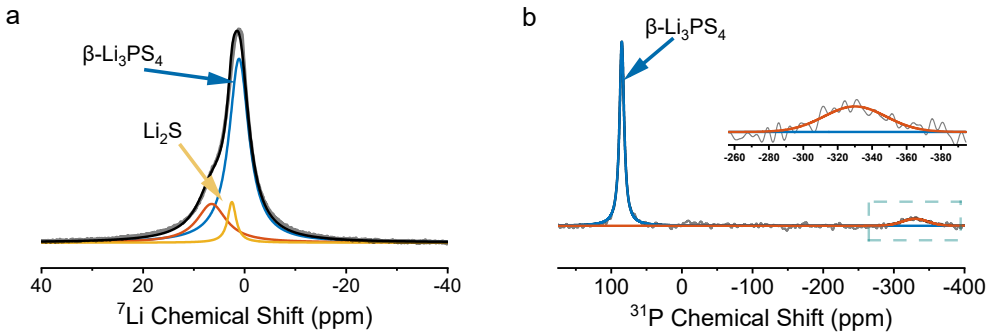

Fig. S13 ss NMR spectra of ^{7}Li (a) and ^{31}P (b) after Li plating for 80 hours at 0.05mA cm^{-2}.

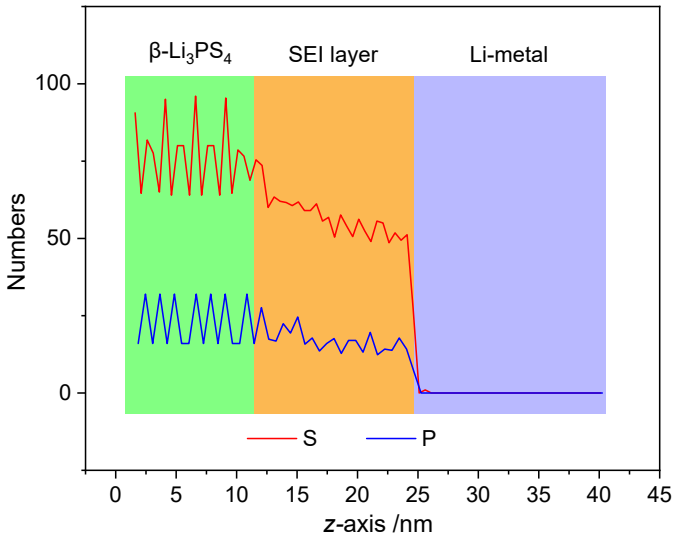

Fig. S14 The counted number of phosphorus and sulfur along the *z*-axis.

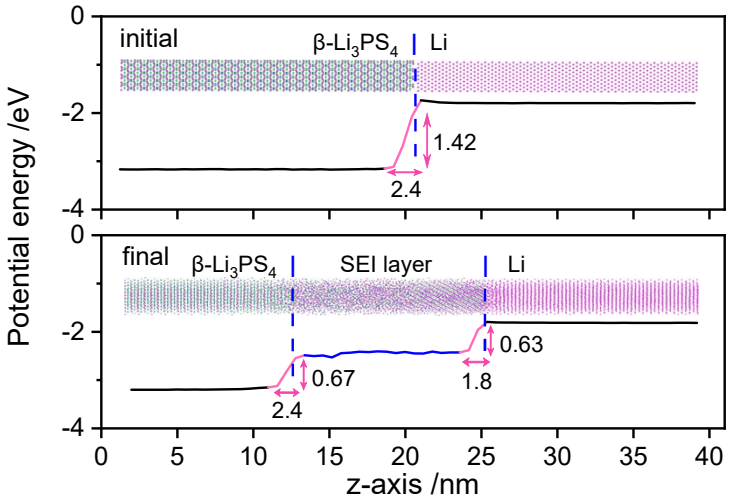

Fig. S15 Potential energy distribution of lithium along the *z*-axis in the (top) initial and (bottom) final interfacial structures.

Table S1. The thickness of the crystalline (Li_2S) region and the SEI layer at different temperatures and pressures of 0 and 100 bar.

T / K	p / bar	Thickness of Li_2S / nm	Thickness of SEI / nm
600	100	8.7	20.6
	0	8.9	21.8
400	100	7.3	14.9
	0	6.7	15.5
300	100	5.0	12.4
	0	5.5	12.9

References

1. F. J. Kresse G, *Phys. Rev. B* **1996**, *54*, 11169.
2. P. E. Blochl, O. Jepsen, O. K. Andersen, *Phys. Rev. B* **1994**, *49*, 16223.
3. P. E. Blochl, *Phys. Rev. B* **1994**, *50*, 17953.
4. H. L. B. Hammer B, J. K. Nørskov, *Phys. Rev. B* **1999**, *59*, 7413.
5. G. M. Dongho Nguimdo, D. P. Joubert, *J. Eur. Phys. B* **2015**, *88*, 1-10.
6. Y. Zhang, H. Wang, W. Chen, J. Zeng, L. Zhang, H. Wang, W. E, *Comput. Phys. Commun.* **2020**, *253*, 107206.
7. H. Wang, L. Zhang, J. Han, W. E, *Comput. Phys. Commun.* **2018**, *228*, 178.
8. L. Zhang, M. Chen, X. Wu, H. Wang, W. E, R. Car, *Phys. Rev. B* **2020**, 102, 041121.
9. L. Zhang, J. Han, H. Wang, R. Car, W. E, *Phys. Rev. Lett.* **2018**, 120, 143001.
10. S. Plimpton, *J. Comput. Phys.* **1995**, 117, 1-19.

11 A. Stukowski, *Modelling Simul. Mater. Sci. Eng.* **2010**, 18, 015012.